and from the US Army (Grant No. DA-ERO-78-G-117). They would also like to thank Dr A. J. Kinloch (Ministry of Defence, PERME) for helpful correspondence and N. L. Bottrell of Westland Helicopters Ltd. for supplying some of the materials.

References

1 Sargent, J. P. and Ashbee, K. H. G. *J. Adhesion* 1980, **11**, 175–189
2 Halpin, J. Cambridge short course on 'Designing with Fibrous Composites', August 1980
3 Sargent, J. P. and Ashbee, K. H. G. *Polymer Composites* 1980, **1**, 93–97
4 Gledhill, R. A., Kinloch, A. J. and Shaw, S. J. *J. Adhesion* 1980, **11**, 3–15
5 Kinloch, A. J. private communication

First results of small and wide angle X-ray scattering of poly(ethylene oxide)/poly(methyl methacrylate) binary blends

Ezio Martuscelli
Istituto di Ricerche su Tecnologia dei Polimeri e Reologia del C.N.R. Arco Felice, Napoli, Italy

and M. Canetti, L. Vicini and A. Seves
Stazione Sperimentale Cellulosa Carta e Fibre Tessili, Milano, Italy
(*Received* 3 *August* 1981; *revised* 6 *November* 1981)

Some preliminary small and wide angle X-ray scattering results are reported from isothermally crystallized samples of poly(ethylene oxide)/(methyl methacrylate) binary blends.

Keywords Analysis; X-rays; X-ray scattering; poly(ethylene oxide); poly(methyl methacrylate); blends; crystallization

Introduction

The crystallization and the thermal behaviour of thin films of poly(ethylene oxide)/poly(methyl methacrylate) (PEO/PMMA) blends obtained by solution casting from chloroform, was investigated by Martuscelli and Demme in a previous work[1]. The results of this study may be summarized as follows:

(i) The dilution of PEO with PMMA causes a depression of the sperulite growth rate. This depression is greater the larger the concentration of non-crystallizing component and the lower the crystallization temperature is.

(ii) The examination, by optical microscopy, of isothermally crystallized thin films of PEO/PMMA blends shows that down to 70% PEO the sample is completely filled with spherulites and no segregation phenomenon of the amorphous component is observed.

(iii) At the same crystallization temperature the observed melting temperature (T_m) of PEO/PMMA blends is lower than that of pure PEO. This effect is more pronounced at lower T_c whilst it is almost negligible at low undercooling.

(iv) For blend samples and for high values of undercooling, T_m increases linearly with T_c. At a well defined value of T_c an abrupt change in the slope is observed. The trend is no longer linear and for lower undercooling the melting point depression tends to disappear.

These observations, together with the finding that in the case of PEO/PMMA blends with high PMMA content the glass transition temperature decreases with increasing PEO content, led the authors to the conclusion that PEO and PMMA are compatible in the melt even if the thermal behaviour of such blends suggests a lower critical solution temperature behaviour below the melting temperature of PEO.

In this communication we report on some preliminary results concerning the analysis of the small and wide angle X-ray scattering of isothermally crystallized samples of PEO/PMMA blends. The main goal of this work is to gain more information about the structure and the overall morphology of such blends by finding some correlation between long spacing, crystal size, composition and crystallization conditions.

Experimental

The characteristics and the source of the polymers are reported in *Table 1*. Films of PEO/PMMA blends were prepared by solution casting from chloroform on glass plates placed on a hot plate set at 50°C. To ensure removal of the solvent the films were kept under vacuum at 70°C for 24 h.

The following compositions were investigated: PEO/PMMA (90/10), (80/20) and (70/30) (w/w).

Table 1 Characteristics of PEO and PMMA

	PEO	PMMA
Source	Fluka AG	BDH
Molecular weight	20000	116000[a]
Melting temperature	65°C	–
Glass transition temperature	−60°C	100°–110°C
Melt flow index (10 Kg)	–	1.0
Melt viscosity 240°C (Shear rate 1120 s^{-1})	–	3.25 K poise

[a] Average viscosity (in chloroform at 25°C)

0032-3861/82/030331-04$03.00

The crystallization conditions used, i.e. crystallization temperature T_c and time, are reported in *Table 2*. The times of crystallization used are sufficiently high to ensure complete crystallization of the samples. Before crystallization the samples were kept for 15 min at 80°C. At lower T_c (45° and 48°C) different crystallization conditions were used for PEO because of its higher rate of crystallization[1].

Small and wide angle X-ray analysis. Small angle X-ray scattering spectra were obtained by means of a Huber 701 camera [Ni filtered CuKα radiation ($\lambda = 1.5418$ Å)]. The scattering intensity was not corrected for the slit smearing effect.

Counting was carried out in a preset count mode accumulating a sufficient number of counts (generally a counting time of 400 s was used). Scanning was done at intervals of 0.01 degrees of 2θ.

To evaluate the periodicity L of the macrolattice formed by the centres of adjacent lamellae of PEO spherulites we applied the Hosemann–Joerchel method which eliminates interparticle interference[2].

For each sample, L was derived from the maximum position in the curves obtained by plotting $\mu^2 \cdot I$ against μ; where $\mu = \frac{2\sin\theta}{\lambda}$ and I is the scattered intensity.

A typical Hosemann–Joerchel plot for PEO/PMMA (90/10) blend is shown in *Figure 1*.

The apparent crystal size L_c of PEO in the direction perpendicular to the (120) crystal plane was calculated with the aid of the Scherrer equation[3]:

$$L_c = \frac{K\lambda}{\beta_0 \cos\theta} \qquad (1)$$

Table 2 Crystallization conditions (T_c = crystallization temperature, t = time of crystallization) used for PEO and its blends with PMMA

T_c (°C)	Time (h)	
−10	rapid quenching	for pure PEO
45	1	for blends
48	3	for blends
	0.25	for PEO
52	6	for blends for PEO
54	24	for blends for PEO

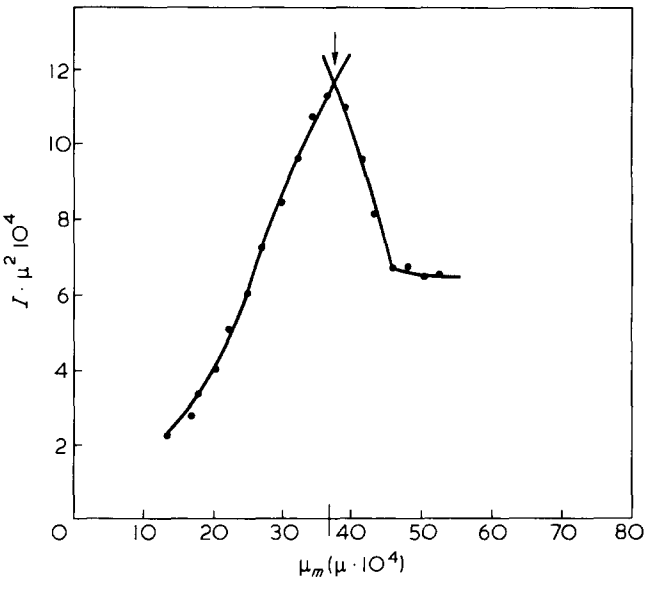

Figure 1 Typical Hosemann–Joerchel plots for PEO/PMMA (90/10) blends

In equation (1) L_c is the crystallite dimension, β_0 is the half-width of the reflection corrected for instrumental broadening and K is approximately unity. In the calculation of L_c no correction for lattice distortion is applied by lack of well-detectable higher-order reflections necessary for this correction to be used.

Wide angle X-ray diffractograms were obtained by means of a SIEMENS (Mod. D500) diffractometer (CuKα radiation).

It is interesting to point out that the (120) planes are the most probable fold planes for PEO lamellae[4]; thus L_c gives a likely measure of the coherent crystal thickness of the lamellar crystal in the growth direction.

Results and Discussion

The values of the distance of the centres of two adjacent lamellae, L, as deduced from the maxima in the Hosemann–Joerchel plots and of the apparent crystal size, as calculated with the aid of the Scherrer equation, are reported in *Table 3* for PEO and its blends with PMMA for different crystallization conditions.

As shown in *Figures 2* and *3*, L increases with T_c and with weight percentage of PMMA for a given blend composition and crystallization temperature, respectively.

Table 3 Values of the distance between the centres of two adjacent lamellae, L, as deduced from the maxima in the Hosemann–Joerchel plots and of the apparent crystal size, L_c, as calculated with the aid of the Scherrer equation, for PEO and its blends with PMMA

	1 h at 45°C		3 h at 48°C		6 h at 52°C		24 h at 54°C	
Sample	L (Å)	L_c (Å)	L (Å)	L_c (Å)	L (Å)	L_c (Å)	L (Å)	L_c (Å)
PEO	170*	220*	170**	400**	275	520	470	745
PEO/PMMA (90/10)	260	220	270	390	295	520	470	475
PEO/PMMA (80/20)	300	275	315	340	370	410	520	355
PEO/PMMA (70/30)	420	355	425	255	465	195	550	165

* These values refer to PEO samples quenched at −10°C. The crystallization at 45°C is not isothermal for PEO because of its high rate of crystallization[1]

** For PEO the time of crystallization at 48°C is 0.25 h in order to avoid annealing effects

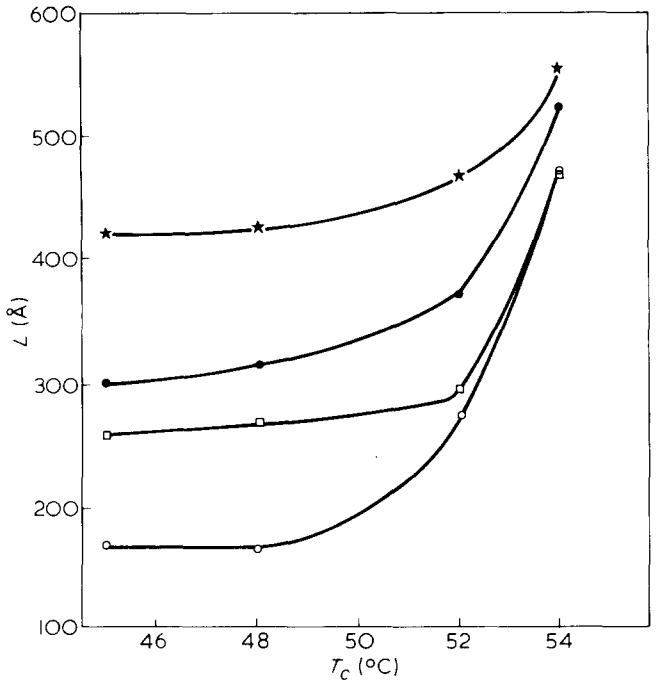

Figure 2 Distance between the centres of two adjacent PEO lamellae (L) as function of crystallization temperature T_c: ○, PEO; □, PEO/PMMA (90/10); ●, PEO/PMMA (80/20); ★, PEO/PMMA (70/30)

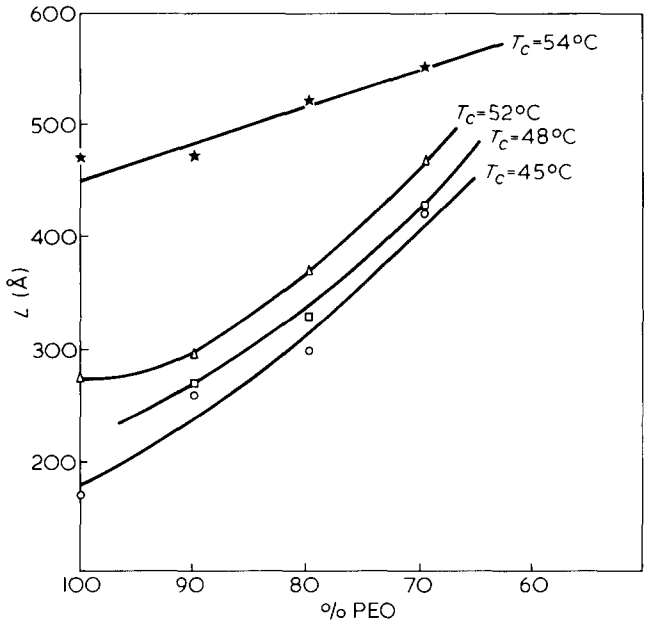

Figure 3 Distance between the centre of two adjacent PEO lamellae (L) as function of blends composition at given T_c: ○, T_c = 45°C; □, T_c = 48°C; △, T_c = 52°C; ★, T_c = 54°C

In a previous work[1] it was found that the equilibrium melting temperature of PEO/PMMA blends decreases with PMMA content. Thus the observed increase of L with PMMA weight percentage at a fixed T_c may be accounted for, at least partially, by the fact that the undercooling is decreased and then, according to the kinetic theory of polymer crystallization, the lamellar thickness should increase[5].

The further observation[1] that no phase separation is observed by optical microscopy in thin films of PEO/PMMA blends isothermally crystallized, was interpreted by the authors as evidence that PMMA molecules are sandwiched in interlamellar regions. This implies that with the percentage of PMMA, the spacing of PEO lamellae should increase in order to accommodate the PMMA molecules. This process is also in agreement with the trend of the curves shown in *Figure 3*.

Plots of the apparent crystal size L_c *versus* blend composition, at given crystallization temperatures, are shown in *Figure 4*.

As can be observed for $T_c > 45$°C PEO spherulites seem to be characterized by crystalline sub-units whose apparent coherent size, along the radial direction, decreases with the PMMA content. This behaviour is probably related to the fact that at higher T_c PEO/PMMA blends separate in the melt into two distinct phases giving size to the formation of PMMA rich domains dispersed in a PEO rich matrix[1]. The presence of these domains and their inclusion in interlamellar regions causes some kind of perturbation hindering the normal growth of the PEO crystals.

The opposite trend observed at $T_c = 45$°C in the curve $L_c \rightarrow$ PEO% is most likely to be accounted for by considering that at this temperature the PEO crystals grow in equilibrium with a one phase melt. Thus the mechanism of PMMA inclusion in interlamellar regions may be different from that at higher temperatures.

The growth process of PEO, from its blends with PMMA, is also complicated by the fact that PMMA molecules, acting as diluent, may cause a decrease in the number of primary and secondary nuclei per unit volume. Furthermore, the possibility for PMMA to induce

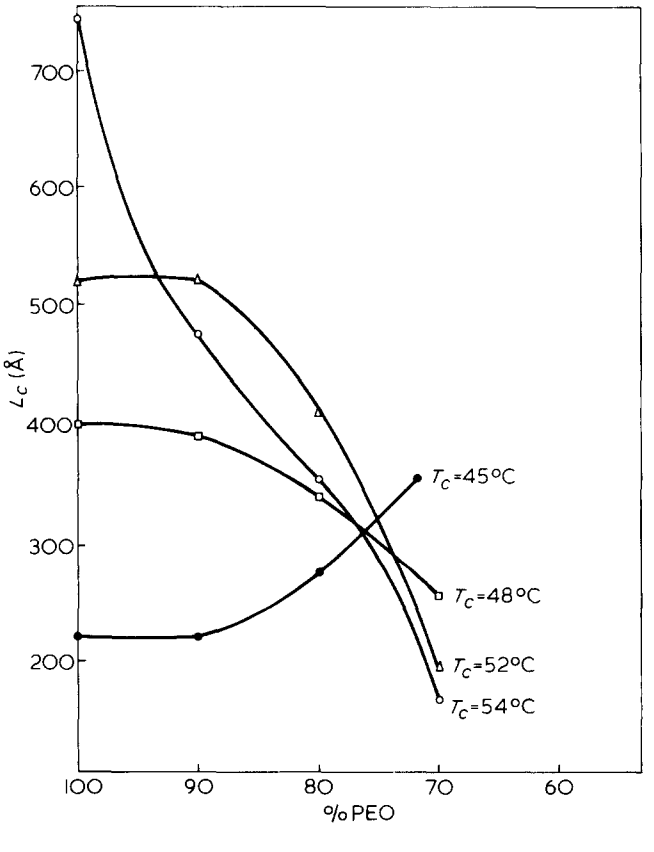

Figure 4 Apparent crystal size (L_c) as function of blends composition at given T_c: ●, T_c = 45°C; □, T_c = 48°C; △, T_c = 52°C; ○, T_c = 54°C

heterogeneous nucleation cannot, in principle, be discarded. The coexistence of all these phenomena make it, at the moment, impossible to give a quantitative explanation of the experimental data presented in this communication.

References

1 Martuscelli, E. and Demma, G. in 'Polymeric blends: Processing-morphology and properties' (Eds. E. Martuscelli, R. Palumbo and M. Kryszewski), Plenum Press, New York, 1980

2 Hosemann, R. and Bagchi, S. N. 'Direct analysis of diffraction by matter', North Holland, Amsterdam, 1962

3 Alexander, L. E. 'X-ray diffraction methods in polymer science', Wiley-Interscience, N.Y., 1969

4 Takahashi, Y. and Tadokoro, H. *Macromolecules* 1973, **6**, 672

5 Hoffman, J. D., Lauritzen, Jr., J. I., Passaglia, E., Ross, G. S., Frolen, L. and Weeks, J. J. *Kolloid Z. Z. Polym.* 1969, **231**, 564

Excluded volume effect on polymer films

A. Baumgärtner

IFF, KFA Jülich, Postfach 1913, 517 *Jülich, W.-Germany*

(*Received* 30 *October* 1981)

Using Monte Carlo methods we have investigated the excluded volume effect on polymer melts in two dimensions. Investigating chain lengths of up to $N=59$ at concentration $c=5/6$, our results strongly support predictions made recently by de Gennes: (1) end-to-end distance and gyration radius exhibit Gaussian behaviour $\propto\sqrt{N}$; (2) but their prefactors differ significantly from their random flight values; (3) in contrast to three-dimensional melts the chains are strongly segregated.

Keywords Polymers; film; melt; excluded volume; hard-sphere model; Monte Carlo simulation; segregation

In a dense system of long flexible polymers each chain is Gaussian and ideal. This was first understood by Flory[1] and has been shown quite convincingly by experiment[2-4], other theoretical argument[5] and computer simulations[6-9].

Recently, de Gennes[5] has put forward some arguments that the 'Flory theorem' does not hold strictly for polymer melts in two dimensions and he expects the chains to be 'not quite ideal and somewhat segregated'. These questions do not seem to have been probed by any method, whether by experiment or computer simulations.

In this communication, we present first Monte Carlo data which strongly support de Gennes' predictions.

As a model, we consider an ensemble of n chains each consisting of $N+1$ pointlike-beads joined together in two dimensions by N rigid links of length l. As an interaction between the beads, we choose a pure hard-core potential, i.e., one has n chains of $N+1$ hard spheres of diameter h each. From recent Monte Carlo renormalization calculations[10], we know that the single hard-sphere polymer chain exhibits the excluded-volume effect most effectively near the fixed point $(h/l)^* \simeq 0.6$. Therefore we choose for our present calculations $h=0.6\ l$. In order to simulate multiple chain systems at fixed concentrations we imposed periodic boundary conditions to our systems[11]. As volume V we choose a rectangular box $V=L^2$ and hence the concentration is defined by $c=nN/(L/l)^2$. Unlike for point-like atoms, any polymer chain will not usually be restricted to just the basic L^2-cell, but may typically extend over two (or more) neighbouring cells. In order to avoid any ambiguity of labelling, we concentrate on that 'image' of the chain for which one coordinate of a bead $\vec{r}_i$ lies within the basic cell. We then consider the interaction between $\vec{r}_i$ and all other beads of the same chain and other chains as well as all images (or parts thereof) of the chains inside the 8 neighbouring cells ('minimum image convention'[11,12]). For computing end-to-end distance and gyration radius of single chains, we have to use the chain not restricted to the basic cell (which then were 'cut into pieces' due to the periodic boundary condition). In order to generate ensembles of chain configurations we used the so-called (reptation dynamic' method for our Monte Carlo simulations[13]. There one first selects one of the ends of the chain at random and then removes the end link of the chain and adds it at the other end, specifying the orientation of the link by the randomly chosen angle φ, in the rante $-\pi<\varphi<\pi$. This mechanism, which corresponds to a movement of the chain along itself, produces an approach towards equilibrium.

Simulations have been performed at concentration $c=5/6$ for several chain lengths of up to $N=59$. In each case, the linear dimension L of the basic cell has been chosen to be $L \gg l\sqrt{N}$, for which the small size of the cell should not affect the chain conformations too much. *Table 1* summarizes our results for the mean-square end-to-end distance $\langle R_N^2\rangle = \langle(\vec{r}_1-\vec{r}_{N+1})^2\rangle$ and the mean-square of gyration $\langle S_N^2\rangle = \sum_{i=1}^{N}\sum_{j=i+1}^{N+1}\langle(\vec{r}_i-\vec{r}_j)^2\rangle/(N+1)^2$. An analysis of these data (*Figure 1*) shows convincingly that both $\langle R_N^2\rangle$ and $\langle S_N^2\rangle$ approach theif Gaussian behaviour $\propto N$ for $N \gtrsim 30$. However, this fact does not mean that the

Table 1 Normalized end-to-end distance and gyration radius at concentration c = 5/6 for various chain lengths and excluded volume ratio h/l = 0.6

$N+1$	n	L/l	R_N^2/l^2N	$\langle S_N^2\rangle/\langle S_N^2\rangle_0$
10	12	12.0	1.81 ± 0.02	1.77 ± 0.02
20	24	24.0	2.01 ± 0.02	1.94 ± 0.02
30	25	30.0	2.06 ± 0.02	2.08 ± 0.02
40	48	48.0	2.10 ± 0.02	2.12 ± 0.02
50	50	54.772	2.12 ± 0.03	2.12 ± 0.03
60	60	65.727	2.11 ± 0.04	2.13 ± 0.04

0032-3861/82/030334-02$03.00